Hexagon structures in a two-dimensional dc-driven gas discharge system

E. Ammelt, Yu. A. Astrov,* and H.-G. Purwins
Institute of Applied Physics, Münster University, Corrensstrasse 2/4, 48149 Münster, Germany
(Received 24 July 1998)

In a dc-driven planar gas discharge semiconductor system, self-organization phenomena have been investigated experimentally. The spatial structures we focus on appear as a spatial modulation of the transversal distribution of the electric current density. These patterns have been observed and recorded through a transparent electrode with spatial resolution via their corresponding light emission. When choosing appropriate experimental conditions, the initially homogeneous current density distribution undertakes a transition to a periodic hexagon and then to a stripe pattern. This behavior of the experimental system is investigated quantitatively and is discussed in the frame of a phenomenological model. [S1063-651X(98)09812-2]

PACS number(s): 47.54.+r, 52.80.−s, 05.60.+w

I. INTRODUCTION

Nonequilibrium spatially extended systems manifest a variety of self-organized patterns [1–4]. Among the different systems in the domain of natural science, a special interest is directed towards pattern-formation phenomena in electronic media. The spreading of research to these subjects is based not only on the intrinsic logic of the development of science. It is believed that principles which govern the behavior of self-organized media can be employed for advanced information processing [5]. The study of pattern formation in electronic media has a rather short history. The main attention in this field has been paid to the investigation of artificial media based on discrete electronic networks, see, e.g., [6], quasi-one-dimensional semiconductor discharge gap systems [7,8], quasi-two-dimensional gas discharge systems which are driven by ac [9] or dc [10–15] voltage, and semiconductor structures [16–22].

We have shown earlier [11] that the planar semiconductor discharge gap structure, which operates at the conditions of a dc-driven low current cryogenic discharge in nitrogen, provides a flexible quasi-two-dimensional electronic medium for studying pattern formation. The essential feature of this experimental object is that electric current can be controlled there interactively, by the amplitude of the feeding voltage and by the intensity of IR light, which irradiates the semiconductor electrode, and thus governs its photoconductivity. Both small-amplitude (harmonic) patterns [11,12] and large-amplitude (solitary) excitations [13–15] can exist in the system in an appropriate range of parameters. It is important to stress that, contrary to ac-driven systems, strictly stationary structures can form in this case. The destabilization of the homogeneous state by the formation of periodic small-amplitude patterns proceeds via the Turing-like scenario [11,12,14,23,24] where transverse coupling of processes that control the current transport in the laterally extended system is involved.

Harmonic (or quasiharmonic) hexagon and stripe stationary patterns are among the basic structures of planar media [25–27]. These patterns are studied in detail for chemical and hydrodynamical systems, see, e.g., [4,28]. Revealing them in a gas discharge system has opened perspectives of the systematic study of pattern-forming properties of planar electronic media. Quantitative peculiarities of the formation of stripe patterns from the homogeneous state in the discussed system have been studied in a previous work [12]. It was experimentally verified that the stripe formation goes via a supercritical bifurcation. Experiments have also revealed that usually slowly drifting stripe patterns can be observed. This phenomenon reflects the absence of strong inhomogeneities in the system that could trap a pattern. At the same time, slight spatial ramps in the system's parameters could initiate the gliding of a pattern across the active area of the system [29].

The main purpose of the present work is to investigate experimentally peculiarities of the transition from a homogeneous state to hexagon patterns. This is interesting from the point of view of the problem of formation of small-amplitude patterns in electronic systems. In this relation the subsequent transition to a stripe pattern is also analyzed. On the other hand, small-amplitude patterns may serve in the considered system as an intermediate stage for the formation of high-amplitude patterns, composed of localized states.

As a procedure for the quantitative evaluation of emerging patterns, a two-dimensional Fourier transformation technique is applied. The seemingly supercritical growth of the amplitude of Fourier components of the hexagon pattern has been shown to be partly related to the spreading of the low-amplitude pattern over the active area of the system while increasing the bifurcation parameter. This effect is connected with the existence of a small but noticeable radial ramp of the physical parameters in the plane of the experimental cell. This gives a gradual increase of current density j from periphery of the discharge area to its center, where its value becomes about 20% higher [12]. That is why, while describing dependences of observed phenomena on electric current, instead of local current density we use its spatially averaged value $\langle j \rangle$.

Due to the indicated ramp in the parameters, the destabilization first occurs in the center, while the bifurcation parameter is increased. Despite this effect, there is left a pronounced hysteretic behavior of the amplitude of the leading

*Also at the A. F. Ioffe Physico-Technical Institute, Russian Academy of Sciences, 194021 St. Petersburg, Russia.

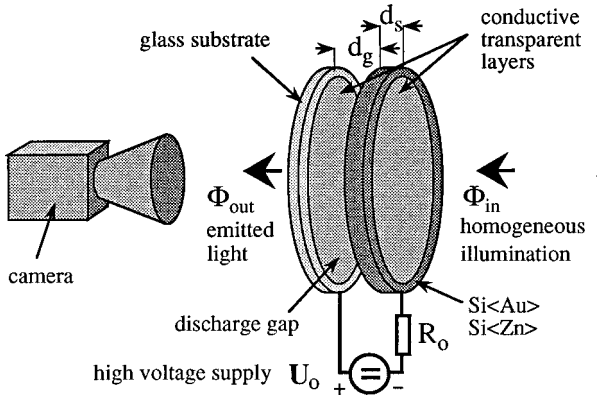

FIG. 1. Experimental setup of the gas discharge system. The discharge gap is enclosed by two planar electrodes. The cathode is made of a photosensitive silicon plate and the anode is transparent to the visible light emitted by the discharge. By illuminating the semiconductor, its specific resistivity decreases. This may be followed by the destabilization of the spatially homogeneous state of the discharge.

mode in the Fourier spectrum when changing the controlling parameter. This is the expected regularity which is specific for transitions from the homogeneous state to a hexagon pattern [25]. The thorough investigation of the transition from hexagon to stripe patterns has not revealed the existence of a hysteresis, while, according to general theoretical results for these transitions in pattern forming media [30], it shall exist. We suppose that this behavior in our case is again due to the mentioned ramp in the system. Finally we try to apply a simple reaction diffusion physical model suggested in [14] for the interpretation of some phenomena reported in the present work.

II. EXPERIMENTAL SETUP

The essential parts of the considered experiment are the same as in previous works [11–15] and is schematically presented in Fig. 1. The system consists of a gas layer, a semiconductor layer serving as cathode, and a transparent anode which is made of the indium tin oxide (ITO) layer covering a glass plate. The anode had a specific plane resistivity of $R_{\square} \approx 150\ \Omega/\square$. The discharge gap is filled with nitrogen at the pressure in the range $p = 60-200$ hPa. As semiconductor material silicon doped with Zn has been used. The total concentration of impurities amounts to $N_{\mathrm{imp}} \approx 10^{16}\,\mathrm{cm}^{-3}$. Nevertheless, it turns out that the type of dopant is not essential: Similar results could be obtained also with use of Au as a dopant of the silicon electrode. To provide a transparent and conductive layer on the outer surface of the silicon wafer, this plane has been homogeneously doped by the implantation technique with B. The layer structure as a whole is cooled with liquid nitrogen down to the temperature $T \approx 90$ K. Due to the cooling, the semiconductor specific resistivity ρ increases up to $\rho = 10^7 - 10^9\,\Omega\,\mathrm{m}$. Because both transparent electrodes, the ITO layer and that on the outer surface of the semiconductor plate, are of a low resistance as compared to resistances of semiconductor and gas discharge domains, they can be considered as equipotential surfaces of the planar structure. The feeding voltage is applied to the described planar structure via highly conductive concentric ring electrodes deposited onto transparent contact layers. The thicknesses of the gas layer d_g and of a silicon plate $d_s \approx d_g \approx 1$ mm, whereas the diameter of the discharge area is in the range 20–22 mm. The dc supply voltage U_0 typically ranges from 1.5 kV up to 3.0 kV and is applied via a load resistor $R_0 = 25\,\mathrm{k}\Omega$ to the electrodes of the planar structure. As the total current usually is not higher than a few tens of microamperes, the voltage drop across the external load R_0 can be neglected. By utilizing the internal photoelectric effect in the IR range, which is provided by the specific doping, the ρ value can be controlled in a well defined manner by illuminating the semiconductor. This feature provides the possibility to modulate ρ spatially and temporally in a rather flexible way. In experiments the cathode layer has been illuminated homogeneously by a thermal (tungsten) light source.

Thus, the discharge state, in particular the total current, can be controlled in a rather broad range. It includes quite low current densities $j \leqslant 1\ \mu A/\mathrm{cm}^2$ where the discharge operates in the Townsend regime. While increasing total current by illuminating the semiconductor cathode or increasing the supply voltage, the density of the charged carriers in the discharge layer increases. This is accompanied by the formation of the net space charge in the discharge gap, and gradually the transition from the Townsend regime to the glow regime takes place [31].

Formation of patterns in the spatial distribution of the current is accompanied by the appearance of corresponding spatial distributions of the glow in the visible range, which is emitted by the discharge. Former investigations of this system [12] have shown that the brightness of the discharge in a good approximation is linearly dependent on the current density of the discharge. Thus, recording emitted light by optical techniques provides an adequate characterization of the spatiotemporal behavior of the current density in the system. The low specific luminosity of nitrogen and the rather low current density necessitate rather sensitive optical instrumentation. In the course of these experiments a CCD camera with a MCP (microchannel-plate) amplifier has been employed. The exposure time δt of this device was sufficiently short ($\delta t \leqslant 50$ ms) with respect to temporal phenomena which have been studied in the described experiments.

III. EXPERIMENTAL RESULTS

The experimental system we investigate exhibits a rather broad range of pattern-formation phenomena as dependent on various system parameters [11–15]. Throughout this paper we consider experimental conditions, where all parameters of the studied structure are constant and spatially homogeneous (if not otherwise indicated $p = 142$ hPa (N_2), $d_g = 0.8$ mm, and $d_s = 1.2$ mm). As controlling parameters, both the illumination density and the supply voltage have been used. In a small range of control parameters, the system responds to changes of one of them in a similar way. Only in a large range of their variation differences may the system's behavior become pronounced. First, we discuss quantitatively the appearance of hexagon patterns. Then we consider the transition from hexagons to striped patterns.

A. Transition to hexagons

In this section we focus on the appearance of a spatially periodic, hexagon modulation of the current density. The re-

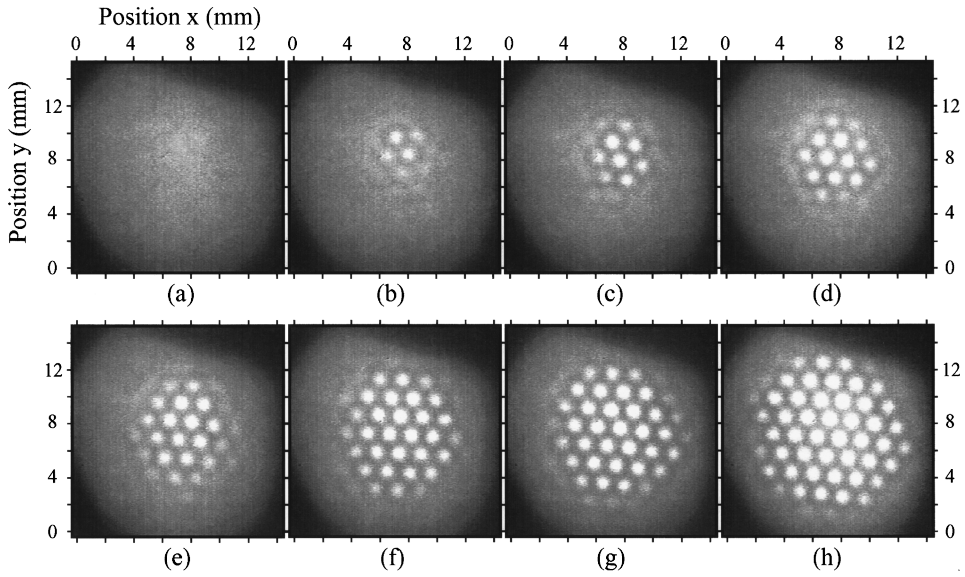

FIG. 2. An example of the gradual evolution of a hexagon pattern while spatially averaged current density in the system rises. Current control is due to the variation in intensity of IR light that irradiates the semiconductor electrode. Brighter areas correspond to increased current density. Notice, that the pattern is not strictly stationary but moves continuously across the active area. $\langle j \rangle$, $\mu A/cm^2$: (a) 5.59; (b) 5.72; (c) 5.79; (d) 6.54. Parameters: $p = 142$ hPa (N_2), $d_g = 0.8$ mm, $d_s = 1.2$ mm, $U_0 = 1.886$ kV.

lated experiments have been carried out by varying the illumination density Φ_{in}, being applied homogeneously to the semiconductor's surface, while all other parameters are kept constant. For the experiments described, the supply voltage was $U_0 = 1.886$ kV. When the illumination density Φ_{in} is low, there is observed a stable spatially homogeneous distribution of current density. Starting from this initial situation, a gradual enhancement in Φ_{in} is accompanied by current increase, while its homogeneous distribution is retained. When exceeding some critical value $\langle j \rangle_{c1}$ of the mean current density $\langle j \rangle$, the homogeneous state is destabilized in favor of a periodic hexagon structure. Further increase of Φ_{in} yields a successively pronounced pattern. A typical example for the evolution of a hexagon pattern is shown in Fig. 2. These images correspond to states of the system with different current density $\langle j \rangle$ while current has been increasing. The distribution of glow reflects the lateral, periodic hexagonal current density distribution with a total number N of spatial periods along one coordinate up to $N \approx 7$. The rather large amount of noise is attributed to the fact that the intensity of the emitted glow is rather low and, therefore, the optical signal had to be amplified. While increasing the controlling parameter further, the system can undergo further transitions, from a hexagonal pattern subsequently to stripe patterns and to zigzag destabilized stripe patterns [13]. We remark that increasing the current in a broad range is generally accompanied by transitions to nonstationary structures [11]. For example, the zigzag instability of stripes appears as the transversal distortion of a stripe propagating along its body [13]. In other scenarios the system can generate spirals and targets, which can also be zigzag destabilized at large amplitude of these patterns [15]. When diminishing the controlling parameter, the entire evolution depicted above passes in the reverse succession and the homogeneous state is restored. The hexagon pattern we have observed in this system exhibits some specific peculiarities which have been found throughout the investigated parameter space: We exclusively have observed H_0 hexagons which can be considered as hexagonal arrangements of spots with increased brightness of discharge, while the system did not show H_π hexagons being complementary patterns to H_0. Another typical property of these hexagons is the fact that they are not strictly stationary, but drift across the active area at rather low velocity, which is about 0.3 mm/sec.

In the following we provide a quantitative analysis of the bifurcation to hexagon patterns. The first estimation is devoted to the symmetry of patterns. For this purpose the image data have been processed by a Fourier transformation with use of the Hanning window, in order to diminish the arbitrary influence of boundaries of the experimental cell on the resulting spectra. A logarithmic representation of the central section of the two-dimensional Fourier transformation of the well developed hexagon pattern of Fig. 2(h) is shown in Fig. 3. Apart from the central peak in the spectrum which

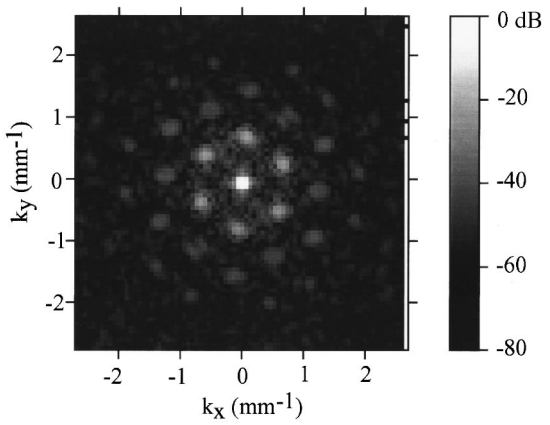

FIG. 3. Fourier spectrum of the hexagon pattern in Fig. 2(h). In order to diminish perturbations of the spectrum by the pattern's boundaries, before making the Fourier transform the image of the pattern was filtered with the Hanning window. Apart from the central peak, six pronounced peaks that represent the hexagon pattern are seen. As a result of nonlinear effects in the formation of periodic spatial structure also higher harmonics rise above the noise level. The picture has been prepared in logarithmic presentation, in order to make clear high-frequency spectral components of small amplitudes that coexist with the large amplitude component at $k = 0$. Amplitudes of the corresponding spectral components can be evaluated using the calibration grey scale bar on the right side of the figure. Parameters: see Fig. 2.

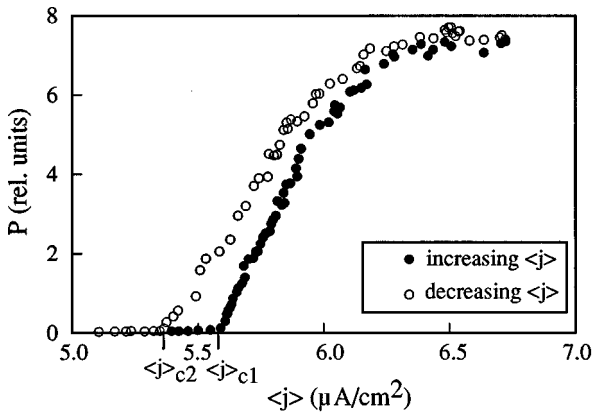

FIG. 4. Total power P of the basic wave number of the hexagon pattern for both increasing and decreasing the control parameter which is current density averaged over the active area $\langle j \rangle$. Under $\langle j \rangle$ increase the pattern evolves from the homogeneous state, when reaching the critical current density $\langle j \rangle_{c1}$. Beyond the bifurcation point the power of the leading wave number increases steadily as a function of the bifurcation parameter until, at $\langle j \rangle \approx 6.5\,\mu A/\mathrm{cm}^2$, its value saturates. When $\langle j \rangle$ is diminished, P also decreases and finally becomes zero at some other critical value $\langle j \rangle_{c2}$. Parameters: see Fig. 2.

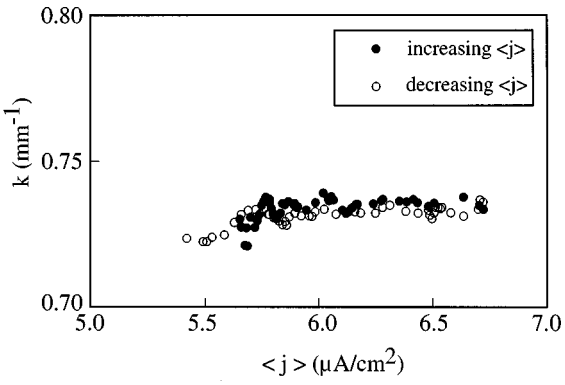

FIG. 5. Wave number of the hexagon pattern as a function of the bifurcation parameter. Parameters: see Fig. 2.

reflects the homogeneous offset, six pronounced peaks at wave number $k \approx 0.73\,\mathrm{mm}^{-1}$, which correspond to the hexagon pattern, can be recognized. The broadening of the peaks is mainly due to the fact that only a few spatial periods are considered ($N \leqslant 7$) and are due to the preprocessing of original spatial distributions by the Hanning window. When characterizing a periodic two-dimensional pattern, an important issue is the angle Ω between adjacent peaks with respect to the origin in k space ($k=0$). The angles have been determined by the following method: For each of the three independent peaks the center of mass has been calculated by considering the contributing vicinity, thus providing a rather high precision of its position in k space. It turns out that in the course of the evolution of the pattern the angle between adjacent peaks is fixed and amounts to $59 \pm 2°$. Deviations from this value become pronounced only at low peak amplitude near the bifurcation point, where the precision of this technique decreases. In the frame of the angle resolution of this method, we can state that we deal with a real hexagon pattern in the total studied range of current density.

We now discuss the magnitude of the pattern while the control parameter changes. A quantitative measure for the intensity of a pattern is given by the total spectral power P yielded by integrating the spectral intensity over all regions in k space which contribute to the pattern under study. In this case we have summarized the intensity for all k values in the radial interval $k = 0.50 - 1.16\,\mathrm{mm}^{-1}$, thus covering the six peaks. The power P as a function of the averaged current density $\langle j \rangle$ is shown in Fig. 4. Starting at some low value of the illumination intensity Φ_{in}, also the current density is low and its distribution is homogeneous. When Φ_{in} is steadily increased, the current density grows, while P at first remains at zero value. Only when $\langle j \rangle$ exceeds some critical value $\langle j \rangle_{c1}$ does P become nonzero and grow monotonously and approximately linearly during a further increase of $\langle j \rangle$. This regularity is observed until the hexagon pattern is rather well developed and saturates. Decreasing Φ_{in} is then followed by the decrease of $\langle j \rangle$. However, the power of the hexagons is retained in a certain range of the current, then the further decrease of $\langle j \rangle$ results in an approximately linear drop of P at the same slope as the growing branch. Finally, a second critical value $\langle j \rangle_{c2}$ is reached, and P becomes equal to zero for smaller values of current. Obviously, the system exhibits a pronounced hysteresis with respect to the creation and annihilation of a hexagon pattern.

The characteristic property of a periodic pattern is its wave number k. In our case of smoothed Fourier spectra it has been estimated by calculating the center of mass of the related peak in the spectra. In order to increase the precision of the method, the mean value of k has been independently calculated for three independent peaks, and then data have been averaged. The wave number as a function of current density is shown in Fig. 5. From these data we conclude that k varies only slightly when the bifurcation takes place. In this context we point out that in the case of the development of stripes a pronounced systematic dependence of the k value on the bifurcation parameter has been revealed [12].

Starting from a well developed hexagon pattern, the further increase in $\langle j \rangle$ due to the enhancement of IR light intensity may initiate different scenarios in the system's evolution, as dependent on parameters: In the case of the hexagon patterns being discussed above, bright spots become successively pronounced and finally they become nonstationary as the resistance of the silicon electrode decreases. By this, the spots undergo a transition from a state where they are strictly embedded in the lattice determined by the hexagon structure to a state where the spots become progressively solitary. In the course of the spots' motion, they interact with each other, and their splitting and merging may be observed. Such patterns evidently contain defects, so the long-range order of the spatial structure is no longer retained. For small deviations of control parameters above the threshold value for the creation of defects, they can be quite isolated, thus being considered as solitary defects in the otherwise perfect structure. An example of a solitary penta-hepta defect in a hexagon pattern is presented in Fig. 6. These pictures show two snapshots of the system's evolution after switching on the feeding voltage. In the development of the hexagon, a stage has been seen in which the pattern had a defect [Fig. 6(a)] that has been cured by the system at a later stage of its evolution [Fig. 6(b)].

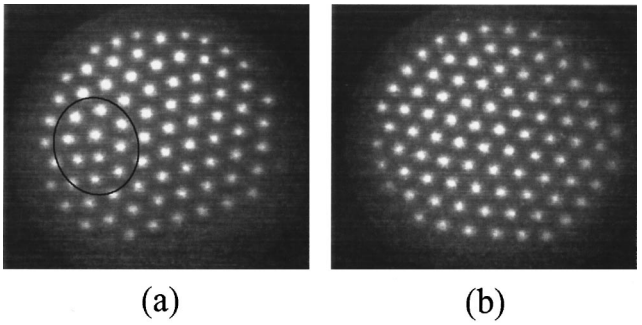

FIG. 6. Observation of a (5+7) defect in a hexagon pattern. Pictures have been taken at different time δt after the supply voltage has been switched on. Defect is seen on (a) inside the marked domain. (a) $\delta t = 1.0$ s, (b) $\delta t = 1.4$ s. Parameters: $p = 129$ hPa (N_2), $d_g = 0.75$ mm, $d_s = 1.2$ mm, $U_0 = 1.9$ kV.

B. Transition from hexagons to stripes

It has been shown earlier [11] that by varying the illumination density Φ_{in}, one is able to observe *hexagon → stripe pattern* transitions. Here, in addition to these prior experiments, we show that also the voltage amplitude U_0 can serve as the control parameter for such a transition, while Φ_{in} is kept constant. Figures 7 and 8 report states of the system for four different stages during the transition from a homogeneous state to a hexagon pattern and finally to a stripe pattern, while increasing U_0. The left-hand column in Fig. 7 represents the spatial light density distributions in patterns while the right-hand column shows the central section of the corresponding two-dimensional Fourier transforms in logarithmic representation. In Fig. 8 the angular distribution of the spectral intensity of the spectra shown in Fig. 7 is represented. For their calculation the radial interval $k = 0.47-1.24$ mm^{-1} in k space has been encountered. This interval has included the main wave numbers, which contribute to the pattern. The angle Ω in Fig. 8 refers to some fixed orientation in k-space axis. We start at low voltage U_0 [Fig. 7(a)] where the system is homogeneous. Accordingly, the spectrum contains a single peak at $k = 0$ and the angular distribution shows some variation at very small amplitude. In the next stage [Fig. 7(b)] a pronounced hexagon pattern in the central region has appeared, and the related spectrum exhibits essentially six peaks. The corresponding angular distribution shows that already at this stage the six peaks are not equal but the amplitude of two peaks significantly exceeds that of the others, thus already announcing the appearance of stripes. In Fig. 7(c), the spatial image reflects the formation of stripes. Starting in the center, bright spots merge in order to form stripes. During this process, stripes in the center and residual hexagons in the outer area apparently coexist. Analogously, the spectrum and the related angular distribution stress the dominance of the stripe pattern with small traces of the hexagon. Finally, the stripe pattern occupies the whole active area [Fig. 7(d)] and the hexagon pattern has totally disappeared. Notice that during current increase the spatial orientation of the stripe pattern could change. This effect is seen when making comparison of angular distributions (c) and (d) of Fig. 8. We remark that the effect of rotation of a stripe pattern by some angle has been observed earlier [12]. It is also worth pointing out that wave numbers for hexagons and stripe patterns are approximately the same

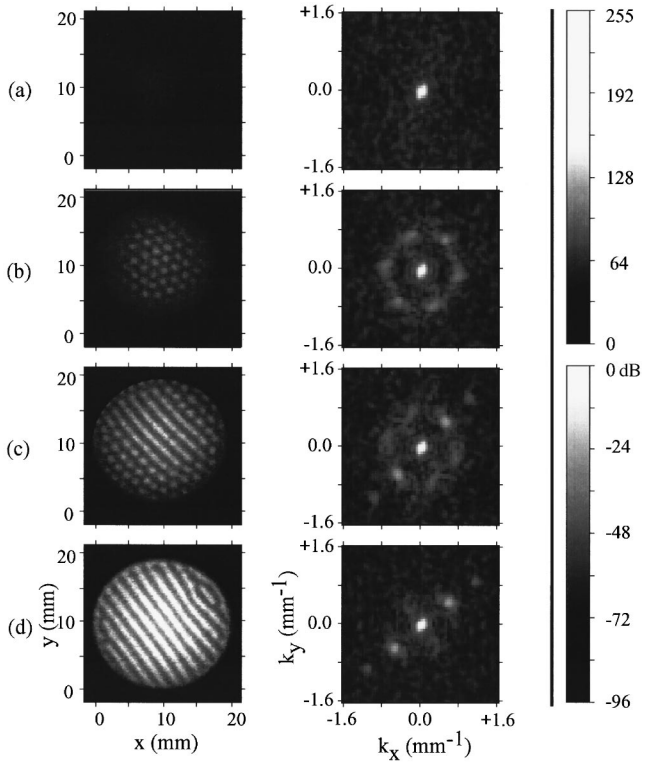

FIG. 7. Transition from a homogeneous state (a) to a hexagon pattern (b) and, via a mixed hexagon/stripe state (c), to a stripe pattern (d). In the left-hand column the spatial light density distribution is represented while the right-hand column reflects corresponding Fourier transforms. This sequence has been achieved by increasing the supply voltage U_0. Parameters: $p = 142$ hPa (N_2), $d_g = 0.8$ mm, $d_s = 1.2$ mm. (a) $U_0 = 1.903$ kV, $\langle j \rangle = 3.10\ \mu A/\text{cm}^2$; (b) $U_0 = 1.940$ kV, $\langle j \rangle = 7.66\ \mu A/\text{cm}^2$; (c) $U_0 = 2.008$ kV, $\langle j \rangle = 12.00\ \mu A/\text{cm}^2$; (d) $U_0 = 2.145$ kV, $\langle j \rangle = 18.21\ \mu A/\text{cm}^2$. Shown on the right-hand side are calibration grey scale bars for spatial distributions (upper bar) and for Fourier spectra (lower bar).

within the accuracy of measurements. Furthermore, it is rather interesting that even in the spectrum of Fig. 8(a) one can observe a rather low signal which is characteristic of a stripe pattern. It evidences the existence of a precursor of the stripe pattern, and indicates the spatial orientation of stripes which will be created by a system at a later stage of its development.

Now we turn to measurements of the variation of the spectral power of patterns in the course of the transitions *homogeneous state→hexagon→stripe pattern* and back. For this purpose the spectral power density has been summed up in the radial interval from $k = 0.47$ to 1.24 mm^{-1}. By this we obtain the total spectral power P of the basic wave numbers which represent the structures we focus on. In particular, this method considers both periodic hexagon and stripe patterns in the same way. The dependence of P on the controlling parameter U_0 is represented in Fig. 9. U_0 covers approximately the same range of the supply voltage as in Fig. 7. Starting at low voltage ($U_0 < 1.900$ kV) the current density distribution is homogeneous. As U_0 exceeds a threshold value U_{0c} ($U_{0c} \approx 1.910$ kV), the transition to the hexagon pattern takes place. This is accompanied by a successive increase of P. At $U_0 \approx 2.000$ kV the hexagon pattern undergoes a transition to periodic stripes while P increases without

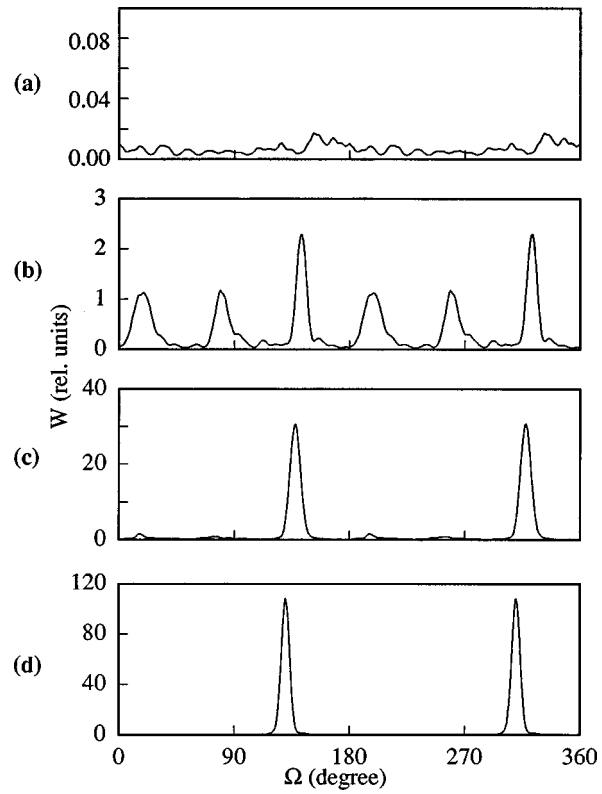

FIG. 8. Angular distributions of power of spectral components in Fourier spectra for different stages of the transition from a homogeneous state (a) to a hexagon pattern (b) and, via a mixed hexagon/stripe state (c), to a stripe pattern (d). The data have been extracted from the corresponding Fourier spectra shown in Fig. 7. k values in the radial range $k=0.47-1.24\,\mathrm{mm}^{-1}$ have been encountered. Notice variation of scales for spectral amplitudes on different plots. Parameters: see Fig. 7.

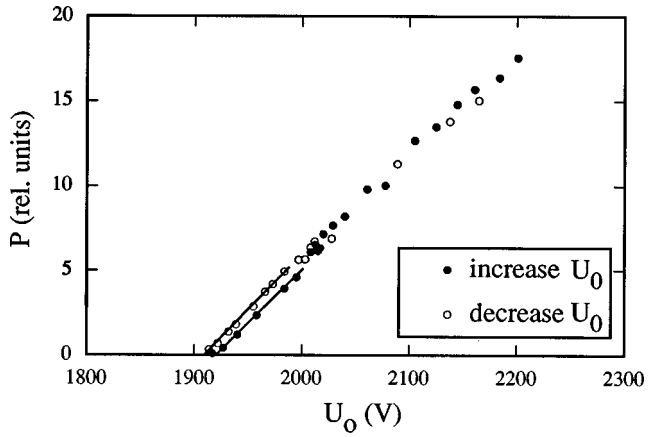

FIG. 9. Power of the leading mode of the pattern as a function of the supply voltage for the scenario shown in Fig. 7. The range of changing U_0 includes transitions from a homogeneous state to a hexagon pattern and, via a mixed hexagon/stripe state, to a stripe pattern. Then U_0 is decreased, and data related to transformations of the pattern in the reverse order are also collected. Note the different values of critical voltages for the appearance and disappearance of the pattern. In order to obtain the power of the leading mode, the range wave numbers with $k=0.47-1.24\,\mathrm{mm}^{-1}$ are analyzed. Parameters: see Fig. 7.

any evident change of its monotonous growth. U_0 is further increased until the stripe pattern is entirely developed [see Fig. 7(d)], then U_0 is gradually diminished and the magnitude of the stripe pattern decreases. After having passed $U_0 \approx 2.030\,\mathrm{kV}$ the stripe pattern decays and the hexagon pattern is successively reconstructed. While diminishing U_0 further, the strength of the hexagon pattern decreases, and finally it vanishes. Throughout the whole range of variation of U_0, the dependence of P on U_0 can be described by a linear fit in a rather good approximation. Only for values of U_0 in the range from $U_0 \approx 1.910$ to 2.000 kV is a pronounced systematic discrepancy between the branches for increasing and decreasing control parameter observed, which can be considered as hysteretic behavior. The related data points are indicated by two linear fits. It is worth pointing out that just this range of the control parameter corresponds to the domain of existence of the hexagon pattern. Too strong scattering of data in Fig. 9 in the domain outside the range of existence of hexagons does not permit us to conclude whether there exists a hysteretic behavior in the transition between hexagons and stripes.

Finally, we notice that both hexagon and stripe patterns exhibit a slow drift over the active space of the experimental system. Estimations of the velocity of the hexagons give the value $v \approx 0.3 \pm 0.1$ mm/s which is on the same order of magnitude as in the former studied case of stripes [12], but is somewhat lower.

IV. INTERPRETATION OF THE OBSERVED PHENOMENA

Bifurcations from a homogeneous state to hexagon or stripe patterns, as well as transitions between them, are well understood theoretically, especially in the case of small-amplitude patterns, where the description with Ginzburg-Landau equations is valid, see e.g., [4,5,34]. In order to understand the peculiarities of a concrete experimental system, it is necessary to reveal the physical mechanisms which control the behavior of the system. In a real highly nonequilibrium system, a number of processes may be important for the formation of patterns. However, even for such complex media as chemical reactors, in some cases it has become possible to extract those degrees of freedom of the system which are important for the understanding of the main features of the observed phenomena; see [35]. A similar problem of constructing a theoretical model exists for the electronic reactor experimentally studied in the present work. Being far from thermal equilibrium and strongly nonlinear, processes in gas discharges are rather complicated for a theoretical description. Discharges in molecular gases, such as nitrogen, are even more complicated as compared with the case of atomic gases, such as Ar or He [31].

Experimentally, the destabilization of the homogeneous distribution of current density and formation of patterns in the device occurs when the transition from the Townsend to the glow mode of the discharge takes place [11–13]. This transition is accompanied by the appearance of a negative differential resistance (NDR) of the discharge gap [31]. It is this process in the system which provides the active properties of the semiconductor-discharge gap pattern-forming media [23,24].

The transition from the Townsend to the glow discharge is due to the influence of space-charge density of ions in the discharge gap on the efficiency of the multiplication of carriers in the gap [31]. That is, the higher the concentration of charge carriers in the gap (correspondingly, the larger the electric current), the more efficient are discharge avalanche processes which support the current transport. At large current density this process may be saturated, and the absolute value of the NDR decreases.

The accumulation of positive ions in the gap has a consequence that the longitudinal electric field, that is, the field along the current, varies in the interelectrode space. The same is true also for densities of charge carriers in the discharge domain. When considering patterning of the current in such a system, one has then inevitably to deal with a 3D representation of physical processes in it. Such variables as local electric field and densities of charge carriers in the gap shall appear in the model. This approach is evidently difficult for a theoretical analysis. In order to simplify a problem, in Ref. [14] it has been supposed that the formation of patterns which are lateral to the current direction can be interpreted on the basis of a 2D model. Such a model can operate with some integral variables of the problem: instead of local electric field E and local densities of charged carriers in the discharge gap, there have been introduced the voltage drop U across the gap

$$U=\int_z E\,dz$$

and the total number of free charge carriers N per unit square:

$$N=\int_z n\,dz,$$

where the corresponding local variables are integrated over the longitudinal coordinate z.

With use of these integral variables, the following two-component reaction-diffusion model has been suggested in Ref. [14] to deal with the pattern-formation problem in the system:

$$\frac{\partial U}{\partial t}=\frac{U_b-U}{\tau_U}-cNU+D_U\Delta U, \tag{1}$$

$$\frac{\partial N}{\partial t}=-\frac{N}{\tau_N}+NU\left[a+b\left(\frac{N}{N+N^*}\right)^2\right]+D_N\Delta N. \tag{2}$$

The first term on the right-hand side of Eq. (1) takes into account the charging of the capacity of the discharge gap by the voltage source U_b. The characteristic time of this process τ_U is determined both by the resistivity of the semiconductor electrode and by capacities of the layered semiconductor discharge gap system [14,32,33]:

$$\tau_U=R_s(C_s+C_g), \tag{3}$$

where R_s is the resistance of a semiconductor electrode, and C_s and C_g are capacities of semiconductor and gas discharge layers, correspondingly. When there is no discharge in the gas domain, its capacity is charged up to the amplitude of the voltage source. In the presence of free carriers in the gap, the rate of its discharging is proportional to the NU product, that is, to the active current in the gap. Constant c determines the efficiency of this process; in our simple model where the conductance of the gas domain is controlled by one kind of carrier having mobility μ, its value is [32,33]

$$c=\frac{e\mu}{\epsilon_0\epsilon_g(1+C_s/C_g)}, \tag{4}$$

where e is the charge of electron, ϵ_0 is the dielectric constant of vacuum, and $\epsilon_g=1$ is the relative dielectric susceptibility of a gas discharge gap.

The second equation deals with dynamics of the density of charge carriers in the gap. The main mechanism of the creation of carriers for discharges with cold electrodes is their avalanche multiplication in electric field. So, when $U=0$, the density of charge carriers decays with a characteristic rate which is controlled by the relaxation time τ_N.

Generation of carriers by electric field is due to positive terms on the right-hand side of Eq. (2). At small N the first of them prevails. For this condition the rate of generation of carriers is proportional to the product NU. This corresponds to the vertical branch of the isocline curve for Eq. (2), that is, the stationary voltage on the discharge gap is not dependent on N. This is the so-called Townsend mode of a self-sustaining discharge [31]. Increasing N is accompanied by the growth of the influence of the second positive term in Eq. (2). This is followed by the dropping in a steady-state U value, as a function of N, which corresponds to a gradual transition to the glow mode of the discharge. In terms of electrical circuits, this is a transition to the NDR of the conductive medium. The value of a specifies the point of crossing the U axis by the isocline of Eq. (2), thus defining the critical voltage $U_c=(\tau_N a)^{-1}$ for the transition from the nonconductive state $N=0$ to the conductive state $N>0$. The parameters b and N^* determine the shape of the isocline curve for Eq. (2) (in other words, the shape of the current voltage characteristic of gas discharge domain for the homogeneous state of the system). Thus, nonlinearities of the model at $\tau_N=\text{const}$ are governed by the parameters a, b, and N^*, which are phenomenological parameters of the model.

The diffusion terms in Eqs. (1) and (2) control the rates of transversal coupling of the variables. As it has been shown in Ref. [14], at a proper set of coefficients the model manifests the transition from a homogeneous state to a hexagon pattern. This transition is of the Turing type, that is, at some (critical) voltage the system becomes unstable against the growth of a mode $k>0$, $i\omega=0$. In its numerical solutions this model has also reproduced the experimentally observed phenomenon of the growth of a hexagon cluster consisting of solitary spots. The development of a cluster proceeds via multiplication of the number of spots (the growth of a dissipative structure via a self-completion scenario); see Ref. [14].

Here, using numerical solutions of Eqs. (1) and (2), we show that this model can also encounter experimentally observed sequence of bifurcations: *homogeneous state* $\rightarrow$ *hexagonal pattern* $\rightarrow$ *stripe pattern*, while increasing the feeding voltage. An example of computed stationary solutions of

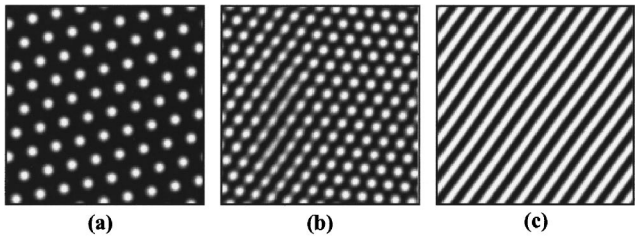

FIG. 10. An example of numerical solutions of the model Eqs. (1) and (2) at increasing the control parameter U_b in the domain of instability of the homogeneous state. Pictures reflect distributions of variable N. Parameters: $\tau_U = 10^{-2}$ sec, $\tau_N = 10^{-3}$ sec, $D_U = 0.625$ cm^2/sec, $D_N = 0.045$ cm^2/sec, $a = 1$, $b = 0.4$, $c = 1.64 \times 10^{-4}$ cm^3/sec, $N^* = 1.5 \times 10^5$ cm^{-3}. Calculations are done on the domain $L \times L$, where $L = 2.72$ cm. (a) $U_b = 1165.0$ V; (b) $U_b = 1205.0$ V; (c) $U_b = 1217.5$ V.

Eqs. (1) and (2) obtained under increasing voltage U_b is shown in Fig. 10. Calculations have been performed for the same set of parameters as in the work [14], where a somewhat more complicated version of the same model has been exploited: Namely, in the cited work there has been included in the equations a global negative feedback where the voltage feeding the two-layer system is dependent on its current.

It is seen from Fig. 10 that, while increasing the control parameter, in the development of the system there is observed a stage where the elements of a hexagonal pattern merge together (b) in order to form periodic stripes (c).

We shall point out, however, that the semiphenomenological model exploited in the present work needs a further refinement. Such an extension shall include the relation between values of phenomenological coefficients in Eqs. (1) and (2) with real microscopic processes that provide nonlinear properties of gas discharge media at conditions of experiments.

V. DISCUSSION AND CONCLUSION

The experimental part of the present work relates to the sequence of transformations in spatial distributions of electric current density inside the discharge domain of a semiconductor discharge gap structure. One essential peculiarity of the experimental object is the slight radial inhomogeneity of the distribution in electric current in the stable domain. This imposes specific features on the observed bifurcation scenarios.

Peculiarities of the growth of the hexagon pattern on the radially ramped area can be followed from the pictures in Figs. 2 and 7. Under increase of the total current at the expense of either increasing the intensity of IR light irradiating the semiconductor electrode (Fig. 2), or increasing the feeding voltage (Fig. 7), the spontaneous destabilization of the system starts in its center where current density is somewhat higher. Then the pattern spreads to the peripheral regions of the experimental system. New maxima of the current distributions build up in the hexagonal arrangement near the existing ones. In this way the hexagon structure grows from the primary current maximum as from a ''seed.'' One of the characteristic properties of these structures is the hysteresis with respect to the magnitude of the pattern when changing the controlling parameter; see Fig. 4. From this fact we draw the conclusion that the transition from the homogeneous state to a hexagon structure has to be considered as a subcritical bifurcation, where the decay of a pattern takes place at a lower value of the bifurcation parameter, as compared to the threshold of its generation.

This subcritical behavior evidently disagrees with the fact that the spectral density P of the leading mode in Fourier spectra of patterns varies steadily in the vicinity of both critical values. This apparent contradiction can be enlightened by the phenomenon just mentioned: Due to the successive spreading of the pattern, the total spectral power of the pattern varies steadily. Only when the sign of the variation of the bifurcation parameter is changed does some hysteresis become evident. Obviously, in this case the occurrence of the hysteresis is related to the spatial spreading of the pattern rather than with the pattern's amplitude as it would be expected in strictly homogeneous systems.

All the patterns observed in the present experiments were not really stationary, instead they were slowly drifting over the area of the system. As it has been discussed earlier [12], this behavior reflects the high quality of the pattern-forming system, in the sense that it has no strong local inhomogeneities which could be able to anchor patterns. It seems, however, that slight gradients of the system's parameters can lift up the translational invariance of the system and cause the movement of the pattern in a definite direction. In this case of noticeable radial gradients of the system's parameters some azimuthal inhomogeneity can remove the rotational invariance of the system. As a result, some definite orientation of patterns in the space of the gas discharge cell and the direction of their movement are chosen by the system.

In the studied system the current flow can be easily varied in two ways: changing either the feeding voltage or the intensity of IR light that irradiates the semiconductor electrode. Both approaches have been used in getting the data. The feeding voltage is a quite natural control parameter for an electrical system. For the case of controlling the structure photoelectrically, one may argue that it would be more appropriate to present data as a function of the intensity of IR light. However, in order to relate explicitly the data on pattern formation with the state of the current-carrying system, for this second case we have used the averaged current density (which is the scaled value of the total current of the device).

To reproduce theoretically transitions between patterns of different spatial symmetry, observed in the experimental system, a two-component semiphenomenological model which takes into account the main physical processes in the system has been applied. Numerical solutions of the model have demonstrated the sequence of bifurcations: *homogeneous state* $\rightarrow$ *hexagonal pattern* $\rightarrow$ *stripe pattern*, while the control parameter (feeding voltage) in the calculations is increased. This behavior, which is a concrete example of the general properties of reaction-diffusion systems [4], is in accordance with experimental results of the present work.

ACKNOWLEDGMENT

The authors acknowledge the support of this work by the Deutsche Forschungsgemeinschaft, Germany.

[1] H. Haken, *Synergetics. An Introduction* (Springer, New York, 1975).
[2] J. D. Murray, *Mathematical Biology* (Springer, Berlin, 1989).
[3] H. Meinhardt, Rep. Prog. Phys. **55**, 797 (1992).
[4] M. C. Cross and P. C. Hohenberg, Rev. Mod. Phys. **65**, 851 (1993).
[5] H. Haken, *Synergetic Computers and Cognition* (Springer, Berlin, 1991).
[6] H.-G. Purwins and C. Radehaus, in *Neural and Synergetic Computers*, edited by H. Haken, Synergetics Vol. 42 (Springer, Berlin, 1988), p. 137.
[7] H. Willebrand, C. Radehaus, F.-J. Niedernostheide, R. Dohmen, and H.-G. Purwins, Phys. Lett. A **149**, 131 (1990).
[8] H. Willebrand, F.-J. Niedernostheide, R. Dohmen, and H.-G. Purwins, in *Cellular Clock Series*, Vol. 5 of Oscillations and Morphogenesis, edited by L. Rensing (Marcel Dekker, New York, 1993), p. 81.
[9] D. G. Boyers and W. A. Tiller, J. Appl. Phys. **41**, 28 (1982); E. Ammelt, D. Schweng, and H.-G. Purwins, Phys. Lett. A **179**, 348 (1993); W. Breazeal, K. M. Flynn, and E. G. Gwinn, Phys. Rev. E **52**, 1503 (1995).
[10] K.-G. Müller, Phys. Rev. A **37**, 4836 (1988).
[11] Yu. Astrov, E. Ammelt, S. Teperick, and H.-G. Purwins, Phys. Lett. A **211**, 184 (1996).
[12] E. Ammelt, Yu. A. Astrov, and H.-G. Purwins, Phys. Rev. E **55**, 6731 (1997).
[13] Yu. A. Astrov, E. Ammelt, and H.-G. Purwins, Phys. Rev. Lett. **78**, 3129 (1997).
[14] Yu. A. Astrov and Yu. A. Logvin, Phys. Rev. Lett. **79**, 2983 (1997).
[15] Yu. A. Astrov, I. Müller, E. Ammelt, and H.-G. Purwins, Phys. Rev. Lett. **80**, 5341 (1998).
[16] E. Schöll, *Nonequilibrium Phase Transitions in Semiconductors* (Springer, Berlin, 1987).
[17] H. Baumann, R. Symanczyk, C. Radehaus, H.-G. Purwins, and D. Jäger, Phys. Lett. A **123**, 421 (1987).
[18] K. M. Mayer, J. Parisi, and R. P. Huebener, Z. Phys. B **71**, 171 (1988).
[19] A. V. Gorbatyuk, I. A. Liniichuk, and A. F. Swirin, Sov. Tech. Phys. Lett. **15**, 224 (1989); A. V. Gorbatyuk and P. B. Rodin, *ibid.* **16**, 519 (1990).
[20] F.-J. Niedernostheide, M. Arps, R. Dohmen, H. Willebrand, and H.-G. Purwins, Physica A **131**, 1085 (1992).
[21] J. Hirschinger, W. Eberle, W. Prettl, F.-J. Niedernostheide, and H. Kostial, Phys. Lett. A **236**, 249 (1997).
[22] Ch. Gossen, F.-J. Niedernostheide, and H.-G. Purwins, in *Nonlinear Dynamics and Pattern Formation in Semiconductors and Devices*, edited by F.-J. Niedernostheide, Springer Proceedings in Physics Vol. 79 (Springer, Berlin 1995), p. 112.
[23] C. Radehaus, R. Dohmen, H. Willebrand, and F.-J. Niedernostheide, Phys. Rev. A **42**, 7426 (1990).
[24] C. Radehaus, H. Willebrand, R. Dohmen, F.-J. Niedernostheide, G. Bengel, and H.-G. Purwins, Phys. Rev. A **45**, 2546 (1992).
[25] F. Busse, J. Fluid Mech. **30**, 625 (1967).
[26] B. A. Malomed and M. I. Tribelskii, Zh. Eksp. Teor. Fiz. **92**, 539 (1987) [Sov. Phys. JETP **65**, 305 (1987)].
[27] S. Ciliberto, P. Coullet, J. Lega, E. Pampaloni, and C. Perez-Garcia, Phys. Rev. Lett. **65**, 2370 (1990).
[28] Q. Ouyang and H. L. Swinney, Nature (London) **352**, 610 (1991).
[29] A. V. Panfilov and J. P. Keener, SIAM (Soc. Ind. Appl. Math.) J. Appl. Math. **55**, 205 (1995).
[30] D. Waldgraef, D. Dewel, and P. Borckmann, Adv. Chem. Phys. **49**, 311 (1982).
[31] Y. P. Raizer, *Gas Discharge Physics* (Springer, Berlin, 1991).
[32] Yu. A. Astrov, A. F. Ioffe Physico-Technical Institute Report No. 1255, 1988 (in Russian).
[33] Yu. A. Astrov, L. M. Portsel, S. P. Teperick, H. Willebrand, and H.-G. Purwins, J. Appl. Phys. **74**, 2159 (1993).
[34] G. H. Gunaratne, Phys. Rev. Lett. **71**, 1367 (1993).
[35] I. Lengyel and I. R. Epstein, Science **251**, 650 (1990).